IOP Conf. Series: Earth and Environmental Science **49** (2016) 022006 doi:10.1088/1755-1315/49/2/022006

Air injection test on a Kaplan turbine: prototype – model comparison

M. Angulo, A. Rivetti, L. Díaz and S. Liscia

Laboratory of Hydromechanics, UNLP, 47 street Nº 200, 1900 La Plata, Argentina

E-mail: mauriangulo@gmail.com

Abstract. Air injection is a very well-known resource to reduce pressure pulsation magnitude in turbines, especially on Francis type. In the case of large Kaplan designs, even when not so usual, it could be a solution to mitigate vibrations arising when tip vortex cavitation phenomenon becomes erosive and induces structural vibrations. In order to study this alternative, aeration tests were performed on a Kaplan turbine at model and prototype scales. The research was focused on efficiency of different air flow rates injected in reducing vibrations, especially at the draft tube and the discharge ring and also in the efficiency drop magnitude. It was found that results on both scales presents the same trend in particular for vibration levels at the discharge ring. The efficiency drop was overestimated on model tests while on prototype were less than 0.2 % for all power output. On prototype, air has a beneficial effect in reducing pressure fluctuations up to 0.2 ‰ of air flow rate. On model high speed image computing helped to quantify the volume of tip vortex cavitation that is strongly correlated with the vibration level. The hydrophone measurements did not capture the cavitation intensity when air is injected, however on prototype, it was detected by a sonometer installed at the draft tube access gallery.

1. Introduction

Large-diameter Kaplan turbines may undergo vibration and erosion at the discharge ring due to the development of tip vortex cavitation phenomena. Severe erosion problems can compromise the lifetime of the machine or cause expensive repair stops. As such issues are difficult to foresee at the design stage, even with the help of CFD simulations and model tests, mitigation strategies have become an important subject. Air injection can be of help in these cases. On the one hand, the reduction of cavitation damage is due to the fact that the presence of a non-condensable gas inside a single cavitation bubble reduces the rate of collapse and increases the minimum bubble volume [1]. On the other hand, it was found recently [2] that miniscule amounts of non-condensable gas (air) into the shear layer of a partial cavity on a wedge could reduce the void fraction (i.e., the ratio of gas to water volumes), thus reducing the potential energy available for noise, vibration and erosion. Air injection has indeed shown potential in preventing erosion due to cavitation in such cases as the chute of spillways of hydroelectric dams [3]. Nevertheless, its application to hydro-turbines remains relatively unexplored and has been mainly confined to the prevention of flow instabilities in Francis turbines due to vortex rope development [4]. Arndt et al. [5] examined the effect of air injection on NACA profiles for the mitigation of cloud cavitation, and found that it was an effective method of minimizing the erosion potential. Consistent results were reported in [6] for an oscillating hydrofoil, where it was also noted that small amounts of air produce a large reduction in noise emission due to cloud cavitation. Rivetti et al. [7, 8] performed

air injection experiments for tip cavitation mitigation on a model scale Kaplan turbine, reaching a reduction of vibration levels at stationary parts of about 50%. Similitude rules for estimating the effect of air in turbine efficiency were developed by Papillon et al. [9, 10] who studied the aeration of vortex cores on a Francis turbine model and prototype.
In this work, air injection experiments on a Kaplan turbine model and prototype are performed. Firstly, the prototype and model scale features, the test procedure and the instrumental are presented. Then, the main results related to vibration reduction, efficiency drop, pressure fluctuation, noise emission and sound levels are summarized. Finally, conclusions about the comparison between model and prototype are given.
The study introduced herein was carried out under the framework of a project focused on the dynamic behavior of Kaplan turbines that combines prototype measurements, model tests and CFD simulations, and is supported by the Yacyretá Binational Entity (EBY), the National University of La Plata, Argentina (UNLP) and the National University of Misiones, Argentina (UNAM).

2. Materials and methods

2.1. Prototype

The focus of this study is set on a five-blade, 9.5-meter-diameter Kaplan turbine, the twelfth unit of the Yacyretá power station located on the Paraná river, at the border between Argentina and Paraguay. The power plant has an installed capacity of 3100 MW (Pe = 155 MW per unit) and operates on a range of heads between 19.5 m and 24.1 m. The rotational velocity of the turbine is 71.42 rpm and its head at the best efficiency point (BEP) is 28 m. The stator has 24 guide and stay vanes. The runner blades have an anti-cavitation lip and the stainless-steel discharge ring extends 0.153 D_p downstream from the runner centerline, Dp being the diameter of the runner. The discharge ring is currently being extended to 0.21 D_p, in order to reduce the impact of cavitation-induced erosion caused by the blade tip vortex.

The aeration device was appended to the auxiliary air supply system of the power station. Air for every unit is provided by compressors through a pipe that runs along the mechanical equipment gallery. By the position of unit #12, a diversion flexible pipe was connected to an 8.5-cubic-meter accumulator tank at a pressure of 8 bars. Two additional accumulation tanks of approximately 1 m^3 of capacity were installed up- and downstream the diversion pipe in order to avoid any probable instabilities in the auxiliary air supply system, with a consequent failure or emergency stop of the units (figure 1. b).

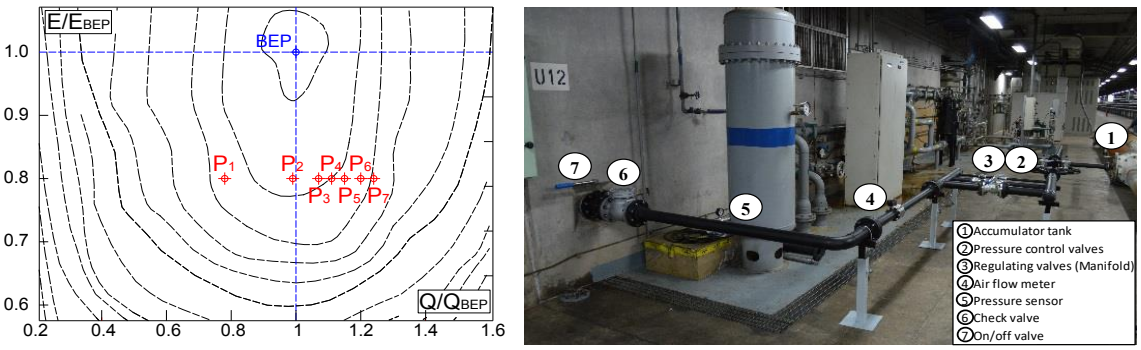

Figure 1. Prototype. Test points on turbine hillchart (a). Air injection device at the mechanical equipment gallery (b).

Air ouflow from the accumulator tank is regulated (up to a maximum of 400 STP lps) by an on/off valve to a 3-inch diameter steel pipe that connects to a manifold controlled by two pressure control valves (set at 4 bars and one is for backup) and on/off valves. Another pipe connects the first manifold to a second one. Each of whose three branches is controlled by a spherical valve (DN

1", 2" and 3"). A 3-inch diameter pipe connects the second manifold to a 2.5-inch diameter pipe to an electronic flowmeter. A manometer and a pressure transducer are attached for the measurement of the inlet pressure. Downstream the flowmeter, there is a 4-inch check valve, to prevent the reversal of water flow when air supply is interrupted, and a 4-inch on/off valve connected to a flange embedded in concrete, for back-up in case of failure or water losses. Further downstream, a 35-meter-long, four-inch diameter pipe connects to a triangular manifold with a cross-section area of 210 cm^2 that surrounds the discharge ring wall. Sixty equidistant 6-millimeter-diameter holes were drilled in the inner wall 0.07 D_p upstream the runner centreline. A more detailed description of the air injection device can be found in [11].

2.2. Scale model

A scaled model of the Kaplan turbine was installed at the test rig of the Laboratory of Hydromechanics of the UNLP (figure 2.a). The facilities allow for the testing of pumps and turbines with a maximum flow rate of 0.9 m^3/s and a maximum head of 40 m. The motor/generator speed and the main circulating pump speed can be controlled by means of a SCADA system in order to set the targeted flow rate and head. Cavitation conditions can be regulated by a vacuum pump and a valve that lower the pressure of the low-pressure tank. Procedures and measurements follow the IEC-60193 standard recommendations. The diameter of the runner is 340 mm and the acrylic discharge ring allows for the visualization of air flow as it develops from the injection section. The rotational velocity of the runner was set at 1000 rpm, ensuring that the Reynolds number is greater than 6.00E+06.

The air injection device consists of an air compressor, a filter of particles and condensed water, a pressure regulating valve, two air flowmeters, a toroidal stainless-steel manifold and twenty pipes with on/off valves connected to 3-millimeter-diameter holes in the discharge ring wall. A ball type air flowmeter was used in the range 0.03 – 0.43 STP lps and another one of spring piston type in the range 0.4 – 2.6 STP lps. A detailed description of these devices can be found in [8].

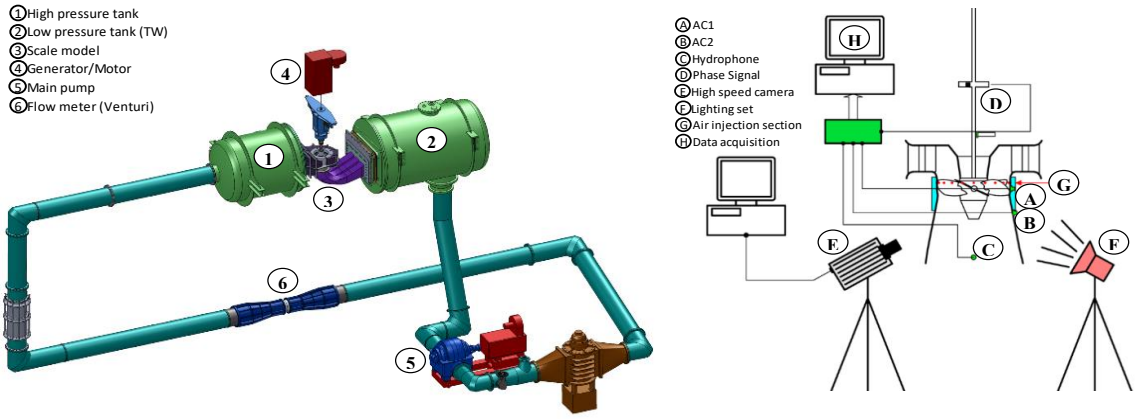

Figure 2. Physical model. Laboratory of Hydromechanics (UNLP) test rig facilities (a). Scheme of the monitoring system and instrumental (b)

2.3 Instrumental

Table 1, summarizes the equipment installed on model and prototype. At figure 2 it can be observed a scheme of the instrumentation and the monitoring system for model tests.
The accelerometer installed on model, at the runner centerline (AC1), give important information due to the proximity to blade tip cavitation area, but this is difficult to implement at prototype regarding that discharge ring is embedded on concrete without a peripheral access gallery. To save this issue an accelerometer was installed at the discharge ring near the man door of the draft tube for both model and prototype, so that a correlation between both accelerometer on model could be correlated.

Table 1. Scale model and Prototype Instrumental.

Instrument	Nomenclature	Characteristics	Prototype	Model
Accelerometer #1	AC1	Brand	Wilcoxon Research	Endevco
		Model	793L	7259B-100
		Position	Shaft guide bearing	Runner C_L
		Range	+/- 10 g	+/- 50 g
		DA frequency	4,200 Hz	35,000 Hz
		Res. freq.	15 kHz	90 kHz
Accelerometer #2	AC2	Brand	Wilcoxon Research	Endevco
		Model	793L	7259B-100
		Position	Discharge ring[1]	Discharge ring[1]
		Range	+/- 10 g	+/- 50 g
		DA frequency	4,200 Hz	35,000 Hz
		Res. freq.	15 kHz	90 kHz
Pressure sensor	PS	Brand	Keller	Kistler
		Model	PAA-21Y	4043A5
		Position	Discharge ring[1]	Runner centerline
		DA frequency	4,200 Hz	35,000 Hz
Air flow Meter	FM	Brand	Testo	Headland / Odin
		Model	6446-DN65mm	H271B / RCP
		Range	6 - 2000 m^3/h	0.40-2.60 lps* / 0.03-0.43 lps*
		Accuracy	3.0 %	2.0 % / 5 %
Hydrophone	HP	Brand	-	Bruel & Kjaer
		Model	-	8103-D-200
		Position	-	Draft tube[2]
		Range (flat)	-	10 - 100 kHz
		DA frequency	-	35,000 Hz
Sonometer	SM	Brand	Bruel & Kjaer	-
		Model	2270 BZ-7222	-
		Position	Discharge ring[3]	-
High Speed Camera	HSC	Brand	-	Photron
		Model	-	SA-4
		Resolution	-	1024x1024 (color)
		Video Speed	-	3600 fps
Data Acquisition system	DAS	Brand	NI	NI
		Model	SCXI-1600 USB	USB-6210
		Inputs	352 analog	16 analog
		Resolution	16 bits	16 bits
		DA frequency	200 kS/s	250 kS/s

[1] 0.30 Dp downstream the runner centerline
[2] 1.00 Dp downstream the runner centerline
[3] At 1 m from the man door and 1 m from ground of access gallery
* STP, standard condition for temperature and pressure (20ºC, 1 atm)

2.4 Test procedure

The test was carried out for 7 power output steps spanning from 0.65 to 1.0 $P_{máx}$ (figure 1.a). At each step, the injected air flow rate, Q_a, (expressed as a fraction of the flow rate at the best efficiency point Q_{BEP}) was gradually increased (from 0.06 ‰ to 0.80‰ in the prototype, from

0.13 ‰ to 2.11 ‰ in the model). Every data point could thus be identified by a combination of power output and injected air flow rate (including no air injection).
The number of steps tested are related with two issues: on the one hand, is to detect the minimum measurable air flow rate able to reduce discharge ring vibrations, which is relevant for the design and implementation of the air injection device at the prototype scale, as a lower flow rate would reduce the size of the compressor and the accumulator tank. On the other hand, the range of air flow rates could be bound at the model scale (it is possible to inject greater amounts of air) so that the tests at the prototype scale could be carried out more efficiently.
At every point, blade tilt angle, guide vane opening, net head, water flow rate, runner speed, water temperature, tailwater level (the pressure at the low-pressure tank, at the model scale) and power output were measured. Air flow rates were measured by means of a computer connected to the air flow meter equipped with Signal Express (Labview) software. Simultaneously, 40-second-long signals of accelerometers, sonometer (at the prototype scale), hydrophone (at the model scale) and pressure sensors, and phase signal data were recorded.
At the prototype scale, once the power output stabilized, the turbine was changed from automate to manual control, blocking the runner and the guide vane positions, in order to prevent the governor from regulating the power output when air is being injected. Before every step, the manifold and the pipe line was dewatered by the injection of a small volume of air (Qa = 0.01 ‰) until the air flow stabilized. With the manifold dewatered, the targeted air flow rate could be injected. Pressure at the outlet of accumulators was checked not to fall under 4 bars, in order to prevent the variation of air flow rates during data acquisition.
At the model scale, the net head remained constant during the test, i.e., E/E_{BEP} = 0.804, and the cavitation conditions reproduced the ones of the power plant as the sigma number of the model was set equal to the sigma plant.
Each power output step represents a different on-cam position of runner blades tilt (β) and guide vanes opening (α), which required the test rig circuit to be stopped. With each start and stop, water was deaerated so that the concentration of dissolved oxygen was less than 5 mg/l. Furthermore, in order to reduce the accumulation of air, the seven air flow rate steps were performed in a short time.

3. Results

Prototype and model tests results were compared in terms of the standard deviation (sd/sd_{max}) of the acceleration registered at the discharge ring accelerometer (AC2), as a function of the air flow rate (figure 3). For both model and prototype, sd_{max} represents the maximum sd of all power output steps. As can be seen, sd/sd_{max} decreases as air flow rate increases although the prototype curve shows a steeper slope. It was inferred from model tests at air flow rates greater than 1.0 ‰ do not entail any significant advantage in the mitigation of vibration.

Furthermore, for lower power outputs (e.g., 0.65 and 0.81 P_{max}), a slight increase in the level of vibration can be observed at the model scale that does not correspond to any visible effect at the prototype scale and the dispersion of the model measurements for flows under 0.50 ‰ is higher than on prototype.

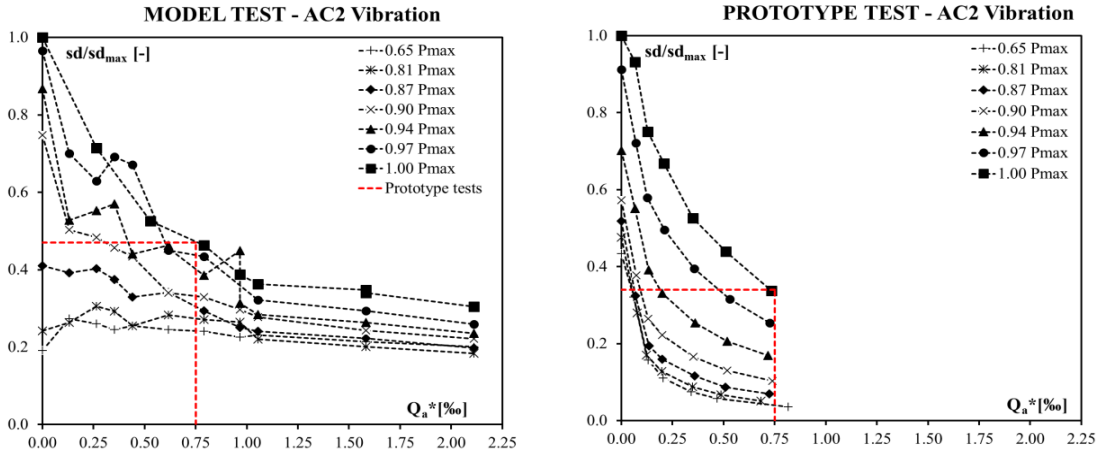

Figure 3. Standard deviation comparison for vibrations at the draft tube AC2 (Discharge ring man door). Model scale (a) Prototype (b)

Analogously, the ratio sd/sd_{max} was recorded at the runner centerline (figure 4.a). Results show good correlation with draft tube vibration.

The hydraulic efficiency loss relative to the no-air flow condition on the model experiments decreases as air flow rate increases (figure 4.b). Losses can reach up to 4 % for the maximum air flow tested, and for the maximum flow tested on prototype can decrease down to 1.5 % and 0.7 % for the best case (0.87 P_{max}). In the case of prototype, the maximum efficiency drop measurable is 0.05 %, in accordance with the instruments sensitivity. A maximum efficiency drop of 0.19 % was measured at the P_{max} step and maximum air flow rate, 0.75 ‰. For flow rates below 0.2 ‰ no efficiency drop was observed.

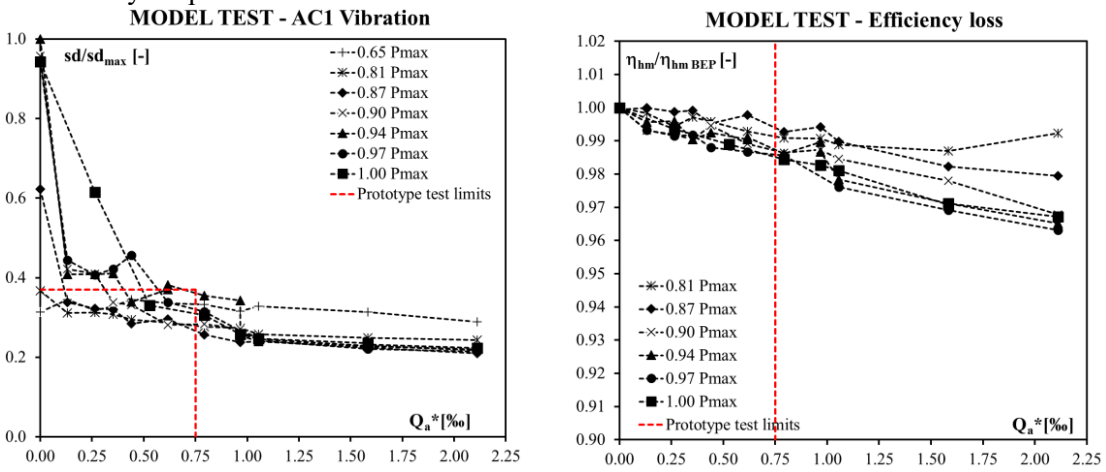

Figure 4. Standard deviation of the level of vibration at the runner centerline (AC1) at model test (a). Relative hydraulic efficiency loss measured on scale model (b)

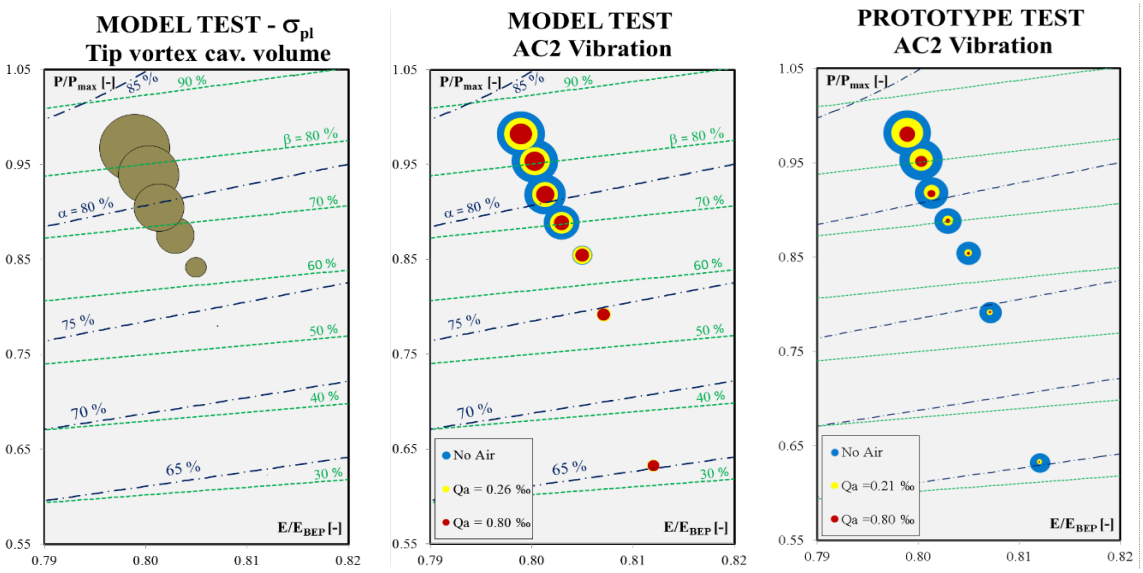

Figure 5. Standard deviation for the level of vibration at the draft tube (AC2) at the model scale (a) and prototype scale (b) for three different air flow rates (0.00 ‰, 0.21 ‰ and 0.80 ‰) as a function of the ratio between a general and the best efficiency point specific energy. Volume of tip vortex cavitation at no-air conditions measured on scale model tests (c). The diameter of the circles is proportional to the level of vibration for the former two and to the volume of cavitation for the latter.

Figure 5, show a hillchart expressed in terms of the ratio between the specific energy (E) and the specific energy at the best efficiency point (E_{BEP}) versus the ratio between a general power output (P) and the maximum power output (P_{max}). It also indicates the blade tilt angle and the guide vane opening relative to the correspondence maximums.

The volume of cavitation at the blade tip, as observed at the model scale by means of speed camera image processing under no–air conditions, is seen to increase as the power output increases (figure 5.a). Indeed, for power outputs below 0.81 P_{max}, the cavitation volume observed is almost imperceptible.

A decrease of the level of vibration was observed as the air flow rate increases at scale model (figure 5.b) and prototype (figure 5.c). Yet, for the two lowest power output steps tested, vibrations remain without significant changes.

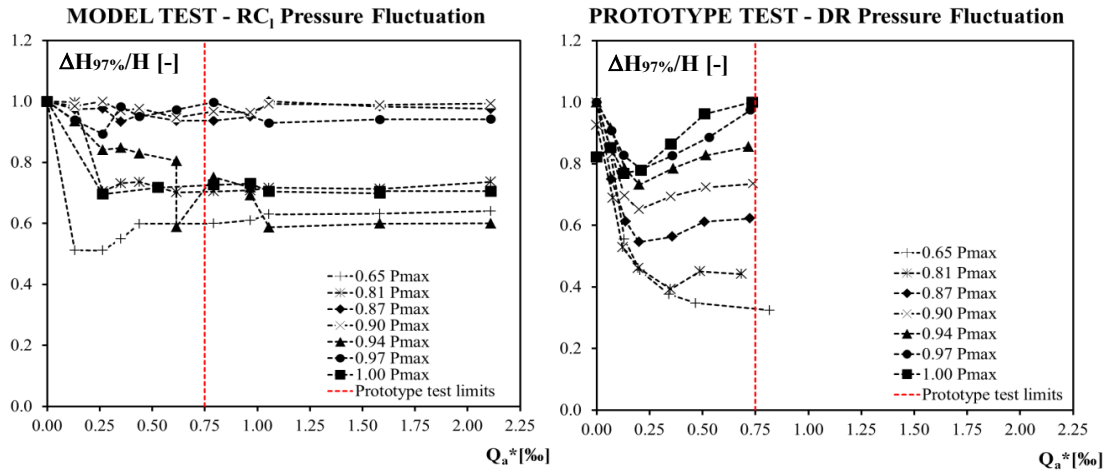

Figure 6. Pressure fluctuation measurements at the runner centerline at model test (a) and at the discharge ring at the prototype (b). For both cases the amplitude of pressure fluctuation ($\Delta H_{97\%}/H$) is relative to the correspondent maximum of each power output step.

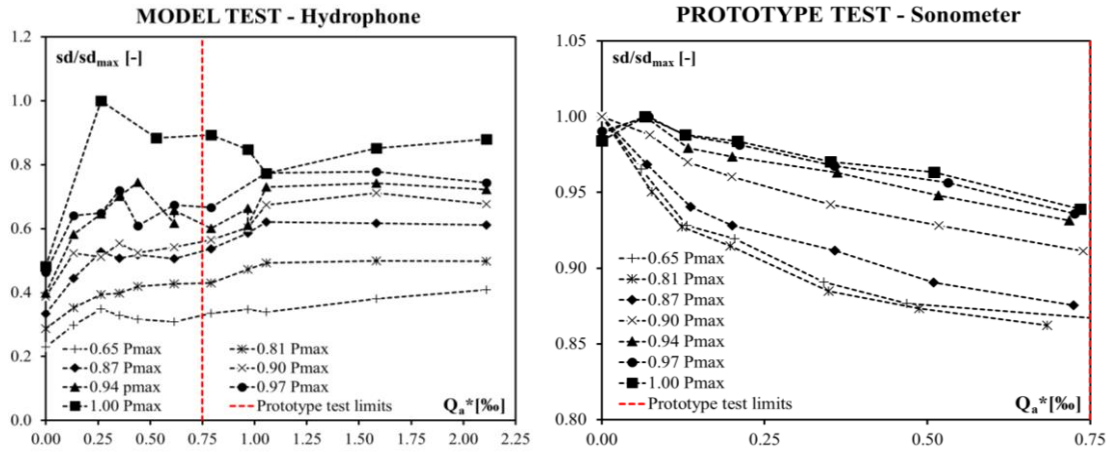

Figure 7. Acoustic emissions measurements at the draft tube at model test (a) and sound levels in the proximity of the draft tube man door access (a).

At prototype, pressure fluctuation at the discharge ring position (figure 6.b) shows a decay for air flow rates below 0.20 ‰, then this tendency is reverted for all the power outputs with the exception of 0.65 $P_{máx}$. At model scale, this trend is not observed at runner centreline position.
Acoustic emissions measured at the draft tube by means of the hydrophone (Figure 7.a) does not capture the decrease of vibrations levels when air is injected, otherwise the sound seems to increase at this position.
Sound levels, captured by the sonometer, near the man door of the draft tube reflects a clear decrease when air flow is injected (figure 7.b), however this was not perceived at the test rig model tests.

4. Discussion and Conclusions

Two parallel tests were carried out on a Kaplan turbine at both model and prototype scales in order to evaluate the beneficial effect of air injection. With the aim of quantifying these effects, measurements of vibration level, pressure fluctuation, turbine efficiency and sound emission were implemented and analyzed.

It was found that air flow injection is an effective way of reducing vibration at the discharge ring of Kaplan turbines as a product of tip vortex cavitation. Model tests showed the same tendency as prototype but on a lower degree. The difference could be due to the different number of injection holes (60 on prototype, 20 on model), that allows for a more uniform and efficient distribution of air on prototype. Therefore, less air flow rates are needed on prototype than on the model.

Even though the maximum amounts of air injected at prototype scale were proportionally lower than at model scale (0.75 ‰ against 2.11 ‰), it is the minimum air flow rate likely to produce any significant effects on the reduction of the level of vibration.

Efficiency drops recorded at model scale were higher than acceptable (in a range of 1-2 %) for air flow rates above 1 ‰. Yet, model tests tend to overestimate the efficiency losses compared against prototype, in which was found to be less than 0.2 % for all cases.

Another important point is that, when no significant volume of tip vortex cavitation is developing, the effect of air, at model scale, may increase or at least have no effect on vibrations. This is important to detect in scale model in order to limit the air injection at lower power outputs. The methodology of computing the cavitation volume (or area) at the blade tip by means of high speed visualization could be helpful to detect such limit.

Regarding to the pressure fluctuations on prototype, the effect of air is beneficial up to certain limits. Beyond this limit, it becomes ineffectual. These trend could not be predicted by scale model.

Finally, measurements of sound near the man door at the draft tube is a good index of the reduction of vibration due to tip vortex cavitation. This might be useful to implement in the power plant due to the simplicity in the instrumentation. On the other hand, the hydrophone is capable of capturing the decrease of cavitation volume without air but, when air is injected, no relation is found related to cavitation mitigation. This may be due to the celerity of sound in water is strongly dependent of the air concentration, and the hydrophone signal is no longer representative of cavitation intensity.

References

[1] Brennen C E 1995 *Cavitation and Bubble Dynamics* (Pasadena: Oxford University Press) p 254
[2] Mäkiharju S A, Ganesh H and Ceccio S L 2015 Effect of Non-Condensable Gas Injection on Cavitation Dynamics of Partial Cavities *J. Phys. Conf. Ser.* **012161** 3–6
[3] Miri M, Nozary N and Kavianpour M R 2015 Experimental Investigation of Flow Aeration on Chute Spillway *Int. J. Therm. Fluid Sci.* **4** 1–8
[4] Papillon B, Sabourin M, Couston M and Deschênes C 2002 Methods for air admission in hydroturbines *XXI IAHR Symp. on Hydraulic Machinery and Systems* (Lausanne)
[5] Arndt R E A, Ellis C R and Paul S 1995 Preliminary Investigation of the Use of Air Injection to Mitigate Cavitation Erosion *Jour. Fluids Eng.* **Vol. 117** 498–504
[6] Reisman G E, Duttweiler M E and Brennen C E 1997 Effect of air injection on the cloud cavitation of a hydrofoil *ASME Fuids Eng. Div. Summer Meet.* **FEDSM97-3249**
[7] Rivetti a, Angulo M, Lucino C and Liscia S 2014 Mitigation of tip vortex cavitation by means of air injection on a Kaplan turbine scale model *IOP Conf. Ser. Earth Environ. Sci.* **22**
[8] Rivetti A, Angulo M, Lucino C and Liscia S 2015 Pressurized air injection in an axial hydro-turbine model for the mitigation of tip leakage cavitation *J. Phys. Conf. Ser.* **656**
[9] Papillon B, Kirejczyk J and Sabourin M 2000 Atmospheric air admission in hydroturbines *Hydrovision* (Charlotte)
[10] Papillon B, Kirejczyk J and Sabourin M 2000 Determination of Similitude Rules for Hydroturbine Aeration *20th IAHR Symp. on Hydraulic Machinery and Systems* (Charlotte)
[11] Rivetti A, Angulo M, Lucino C, Hene M, Capezio O and Liscia S 2016 Implementation of pressurized air injection system in a Kaplan prototype for the reduction of vibration caused by tip vortex cavitation *28th IAHR Symp. on Hydraulic Machinery and Systems* (Grenoble)

Acknowledgement

The authors would like to thanks to the technical director of the Yacyretá power station, Eng. Oscar Capezio, and the personal of the regulation department for their important contribution. Special thanks to Martín Zagaglia, for his collaboration in the execution of the model tests.